Original Article

The Leptin-Deficient (*ob/ob*) Mouse

A New Animal Model of Peripheral Neuropathy of Type 2 Diabetes and Obesity

Viktor R. Drel, Nazar Mashtalir, Olga Ilnytska, Jeho Shin, Fei Li, Valeriy V. Lyzogubov, and Irina G. Obrosova

Whereas functional, metabolic, neurotrophic, and morphological abnormalities of peripheral diabetic neuropathy (PDN) have been extensively explored in streptozotocin-induced diabetic rats and mice (models of type 1 diabetes), insufficient information is available on manifestations and pathogenetic mechanisms of PDN in type 2 diabetic models. The latter could constitute a problem for clinical trial design because the vast majority of subjects with diabetes have type 2 (non–insulin dependent) diabetes. This study was aimed at characterization of PDN in leptin-deficient (*ob/ob*) mice, a model of type 2 diabetes with relatively mild hyperglycemia and obesity. *ob/ob* mice (~11 weeks old) clearly developed manifest sciatic motor nerve conduction velocity (MNCV) and hind-limb digital sensory nerve conduction velocity (SNCV) deficits, thermal hypoalgesia, tactile allodynia, and a remarkable (~78%) loss of intraepidermal nerve fibers. They also had increased sorbitol pathway activity in the sciatic nerve and increased nitrotyrosine and poly(ADP-ribose) immunofluorescence in the sciatic nerve, spinal cord, and dorsal root ganglion (DRG). Aldose reductase inhibition with fidarestat (16 mg · kg^{-1} · d^{-1}), administered to *ob/ob* mice for 6 weeks starting from 5 weeks of age, was associated with preservation of normal MNCV and SNCV and alleviation of thermal hypoalgesia and intraepidermal nerve fiber loss but not tactile allodynia. Sciatic nerve nitrotyrosine immunofluorescence and the number of poly(ADP-ribose)–positive nuclei in sciatic nerve, spinal cord, and DRGs of fidarestat-treated *ob/ob* mice did not differ from those in nondiabetic controls. In conclusion, the leptin-deficient *ob/ob* mouse is a new animal model that develops both large motor and sensory fiber and small sensory fiber PDN and responds to pathogenetic treatment. The results support the role for increased aldose reductase activity in functional and structural changes of PDN in type 2 diabetes. *Diabetes* 55: 3335–3343, 2006

From the Pennington Biomedical Research Center, Louisiana State University System, Baton Rouge, Louisiana.

Address correspondence and reprint requests to Irina G. Obrosova, PhD, Pennington Biomedical Research Center, Louisiana State University, 6400 Perkins Rd., Baton Rouge, LA 70808. E-mail: obrosoig@pbrc.edu.

Received for publication 29 June 2006 and accepted in revised form 31 August 2006.

AR, aldose reductase; DRG, dorsal root ganglion; INFD, intraepidermal nerve fiber density; MNCV, motor nerve conduction velocity; PDN, peripheral diabetic neuropathy; SNCV, sensory nerve conduction velocity; TBS, Tris-buffered solution.

DOI: 10.2337/db06-0885

Peripheral diabetic neuropathy (PDN) is a devastating complication of diabetes and a leading cause of foot amputation (1,2). Clinical indications of PDN include increased vibration and thermal perception thresholds that progress to sensory loss, occurring in conjunction with degeneration of all fiber types in the peripheral nerve. A proportion of patients with PDN also describe abnormal sensations such as paresthesias, allodynia, hyperalgesia, and spontaneous pain that sometimes coexist with loss of normal sensory function (3). Functional, metabolic, neurotrophic, and morphological abnormalities of PDN have extensively been explored in animal models of type 1 diabetes and, in particular, in streptozotocin-induced diabetic rats (4–8) and mice (9,10). In contrast, manifestations and pathogenetic mechanisms of PDN in type 2 diabetic models remain remarkably understudied despite the fact that the vast majority of subjects with diabetes have type 2 (non–insulin dependent) diabetes.

The epidemic of obesity in the developed countries is driving a large increase in type 2 diabetes and consequentially setting the scene for an impending wave of morbidity and mortality associated with diabetes complications including PDN (11). The latter dictates a necessity for detailed studies of neuropathic changes in animal models of PDN resulting from obesity and type 2 diabetes. Important information on neurological and neurovascular deficits characteristic for PDN has been obtained in studies in Zucker obese and Zucker diabetic fatty rats (12,13) and other models of PDN of type 2 diabetes (14–16). Here, we describe PDN in leptin-deficient (*ob/ob*) mice, a model of obesity and mild type 2 diabetes (17,18) that is clearly characterized by manifest motor and sensory nerve conduction deficits, small sensory nerve fiber neuropathy, intraepidermal sensory nerve fiber loss, and oxidative-nitrosative stress in peripheral nerve, spinal cord, and dorsal root ganglion (DRG). These neuropathic changes (except tactile allodynia) appeared amenable to pathogenetic treatment with the aldose reductase (AR) inhibitor fidarestat (19), which supports the role for increased AR activity in PDN associated with obesity and mild type 2 diabetes.

RESEARCH DESIGN AND METHODS

Unless otherwise stated, all chemicals were of reagent-grade quality and were purchased from Sigma Chemical (St. Louis, MO). Rabbit polyclonal anti-

TABLE 1
Initial and final body weights and blood glucose concentrations in nondiabetic control mice and *ob/ob* mice with and without fidarestat treatment

	Body weight (g)		Blood glucose (mmol/l)	
	Initial	Final	Initial	Final
Control	20.6 ± 0.40	29.0 ± 0.95	7.9 ± 0.17	8.0 ± 0.20
Control + F	20.4 ± 0.49	28.0 ± 1.10	8.6 ± 0.28	8.1 ± 0.31
ob/ob	46.9 ± 0.95*	57.1 ± 1.36*	18.8 ± 2.16*	17.6 ± 1.77*
ob/ob + F	46.6 ± 0.84*	57.9 ± 1.03*	19.0 ± 2.32*	15.9 ± 2.83*

Data are means ± SE; n = 12–21 per group. *Significantly different from nondiabetic controls ($P < 0.01$). F, fidarestat.

nitrotyrosine antibody was purchased from Upstate (Lake Placid, NY) and mouse monoclonal anti-poly(ADP-ribose) from Trevigen (Gaithersburg, MD). Secondary Alexa Fluor 488 goat anti-rabbit and Alexa Fluor goat anti-mouse antibodies, as well as Prolong Gold Antifade Reagent, were purchased from Invitrogen (Eugene, OR). Avidin/Biotin Blocking kit, MOM Basic kit, VECTASTAIN Elite ABC kit (Standard), DAB Substrate kit, and 3,3′-diaminobenzidine were obtained from Vector Laboratories (Burlingame, CA). Rabbit polyclonal anti-protein gene product 9.5 (ubiquitin c-terminal hydrolase) antibody was purchased from Chemicon International (Temecula, CA). Other reagents for immunohistochemistry were purchased from Dako Laboratories (Santa Barbara, CA).

The experiments were performed in accordance with regulations specified by the National Institutes of Health *Principles of Laboratory Animal Care* (1985 revised version) and Pennington Biomedical Research Center Protocol for Animal Studies. Four-week-old C57Bl6 mice and leptin-deficient C57Bl6/J *ob/ob* mice were fed a standard mouse diet (PMI Nutrition International, Brentwood, MO) and had access to water ad libitum. Blood samples for glucose measurements were taken from the tail vein at the beginning of the study and the day before the animals were killed. The *ob/ob* mice with blood glucose >13.8 mmol/l were considered to have diabetes. The experimental groups comprised control and *ob/ob* mice treated with or without the AR inhibitor fidarestat (16 mg · kg^{-1} · d^{-1}). The treatment was started at 5 weeks of age and continued for 6 weeks. The physiological and behavioral tests have been performed in the following order: tactile responses to flexible von Frey filaments (1st day), thermal algesia (2nd day), and sensory nerve conduction velocity (SNCV) and motor nerve conduction velocity (MNCV) (3rd day). Measurements of MNCV and SNCV were performed in mice anesthetized with a mixture of ketamine and xylazine (45 and 15 mg/kg body wt i.p., respectively).

Anesthesia, euthanasia, and tissue sampling. The animals were sedated by CO_2 and immediately killed by cervical dislocation. One sciatic nerve from each mouse was rapidly dissected and frozen in liquid nitrogen for subsequent assessment of sorbitol pathway intermediates. Another sciatic nerve, spinal cord, DRGs, and foot pads were fixed in normal buffered 4% formalin for assessment of nitrotyrosine and poly(ADP-ribose) by immunofluorescent histochemistry.

Physiological tests. Sciatic MNCV and hind-limb digital SNCV have been measured as we have described elsewhere (9). In all measurements, body temperature was monitored by a rectal probe and maintained at 37°C with a warming pad. Hind-limb skin temperature was also monitored by a thermistor and maintained between 36 and 38°C by radiant heat.

Behavioral tests. Tactile responses were evaluated by quantifying the withdrawal threshold of the hindpaw in response to stimulation with flexible von Frey filaments as we have described (20). The paw withdrawal latency in response to the radiant heat (15% intensity, cutoff time 30 s) was determined as we have described (20).

Immunohistochemical studies. All sections were processed by a single investigator and evaluated blindly. Low-power observations of skin sections stained for protein gene product 9.5 were made using a Zeiss Axioskop microscope. Color images were captured with a Zeiss Axiocam HRc charged-coupled device camera at 1,300 × 1,030 resolution. Low-power images were generated with a 40× acroplan objective using the automatic capturing feature of the Zeiss Axiovision software (version 3.1.2.1). Low-power observations of sciatic nerve, spinal cord, and DRG sections stained for nitrotyrosine and poly(ADP-ribose) were made using a Zeiss Axioplan 2 imaging microscope. Color images were captured with a Photometric CoolSNAP$_{HQ}$ charged-coupled device camera at 1,392 × 1,040 resolution. Low-power images were generated with a 40× acroplan objective using the RS Image 1.9.2 software.

Nitrotyrosine immunoreactivity in sciatic nerve, spinal cord, and DRG neurons. Nitrotyrosine immunoreactivity in the sciatic nerve, spinal cord, and DRG neurons was assessed by immunofluorescent histochemistry. In brief, sections were deparaffinized in xylene, hydrated in decreasing concentrations of ethanol, and washed in water. For immunofluorescent histochemistry, rabbit polyclonal anti-nitrotyrosine antibody was used in a working dilution of 1:400. Secondary Alexa Fluor 488 goat anti-rabbit antibody was applied in a working dilution 1:200. Sections were mounted in Prolong Gold Antifade Reagent. The intensity of fluorescence was graded from 1 to 4 (1, no staining; 2, faint; 3, moderate; and 4, intense), and the immunohistochemistry score was expressed as mean ± SE for each experimental group.

Poly(ADP-ribose) immunoreactivity. Poly(ADP-ribose) immunoreactivity was assessed as described (9), with minor modifications. In brief, sections were deparaffinized in xylene, hydrated in decreasing concentrations of ethanol, and washed in water. Nonspecific binding was blocked with the mouse immunoglobulin blocking reagent supplied with the Vector MOM Basic Immunodetection kit. Then, mouse monoclonal anti–poly(ADP-ribose) antibody was diluted 1:100 in 1% BSA in Tris-buffered solution (TBS) and applied overnight at 4°C in the humidity chamber. Secondary Alexa Fluor 488 goat anti-mouse antibody was diluted 1:200 in TBS and applied for 2 h at room temperature. Sections were mounted in Prolong Gold Antifade Reagent. At the least, 10 fields of each section were examined to select 1 representative image. Representative images were microphotographed and the number of poly-(ADP-ribose)–positive nuclei calculated for each microphotograph.

Intraepidermal nerve fiber density. Intraepidermal nerve fiber density (INFD) was assessed as described (21) with minor modification. Three randomly chosen 5-μm sections from each mouse were deparaffinized in xylene, hydrated in decreasing concentrations of ethanol, and washed in water. Nonspecific binding was blocked by 10% goat serum containing 1% BSA in TBS (Dako, Carpinteria, CA) for 2 h using the Avidin/Biotin Blocking kit according to the manufacturer's instructions. Then, rabbit polyclonal anti-protein gene product 9.5 (ubiquitin c-terminal hydrolase) antibody was applied in 1:2,000 dilution. Secondary biotinylated goat anti-rabbit IgG (H+L) antibody was applied in 1:400 dilution and the staining performed with the VECTASTAIN Elite ABC kit (Standard). For visualization of specific binding sites, the DAB Substrate kit containing 3,3-diaminobenzidine was used. Sections were counterstained with Gill's hematoxylin, dehydrated, and mounted in Micromount mounting medium (Surgipath Medical, Richmond, IL). Intraepidermal nerve fiber profiles were counted blindly by three independent investigators, under an Olympus BX-41 microscope, and the average values were used. Microphotographs of stained sections were taken on an Axioscop 2 microscope (Zeiss) at 4× magnification, and the length of epidermis was assessed with the ImagePro 3.0 program (Media Cybernetics). Mean ± SE of the sample length (2.8 ± 0.3 mm) was investigated to calculate a number of nerve fiber profiles per millimeter of epidermis.

Biochemical studies. Glucose, sorbitol, and fructose concentrations in sciatic nerve have been spectrofluorometrically assessed by enzymatic procedures with hexokinase/glucose 6-phosphate dehydrogenase, sorbitol dehydrogenase, and fructose dehydrogenase, as we described elsewhere (22).

Statistical analysis. The results are expressed as means ± SE. Data were subjected to equality of variance F test and then to log transformation, if necessary, before one-way ANOVA. Where overall significance ($P < 0.05$) was attained, individual between-group comparisons were made using the Student-Newman-Keuls multiple range test. Significance was defined at a P value <0.05. When between-group variance differences could not be normalized by log transformation (datasets for body weights and plasma glucose), the data were analyzed by the nonparametric Kruskal-Wallis one-way ANOVA, followed by the Bonferroni/Dunn test for multiple comparisons.

RESULTS

Both initial and final body weights and initial and final blood glucose concentrations were higher in *ob/ob* mice compared with nondiabetic controls (Table 1). Fidarestat

TABLE 2
Sciatic nerve sorbitol pathway intermediate concentrations (in nanomoles per milligram wet weight) in nondiabetic control and diabetic *ob/ob* mice with and without fidarestat treatment

	Glucose	Sorbitol	Fructose
Control	2.20 ± 0.35	0.092 ± 0.021	0.404 ± 0.162
Control + F	2.23 ± 0.42	0.067 ± 0.033	0.343 ± 0.157
ob/ob	20.8 ± 2.0*	0.196 ± 0.035†	3.34 ± 0.40*
ob/ob + F	21.5 ± 3.4*	0.099 ± 0.031‡	0.903 ± 0.25§

Data are means ± SE; n = 8–10. Significantly different from nondiabetic controls (*$P < 0.01$ and †$P < 0.05$). Significantly different from untreated *ob/ob* mice (‡$P < 0.05$ and §$P < 0.01$). F, fidarestat.

did not affect weight gain or blood glucose concentrations in either nondiabetic control or *ob/ob* mice.

Sciatic nerve glucose, sorbitol, and fructose concentrations were increased in *ob/ob* mice compared with controls (Table 2). Fidarestat treatment did not affect sciatic nerve glucose concentrations but essentially prevented an increase in sorbitol and fructose concentrations in *ob/ob* mice. Sciatic MNCV was 16% lower in untreated *ob/ob* mice compared with nondiabetic controls (Fig. 1*A*). In contrast,

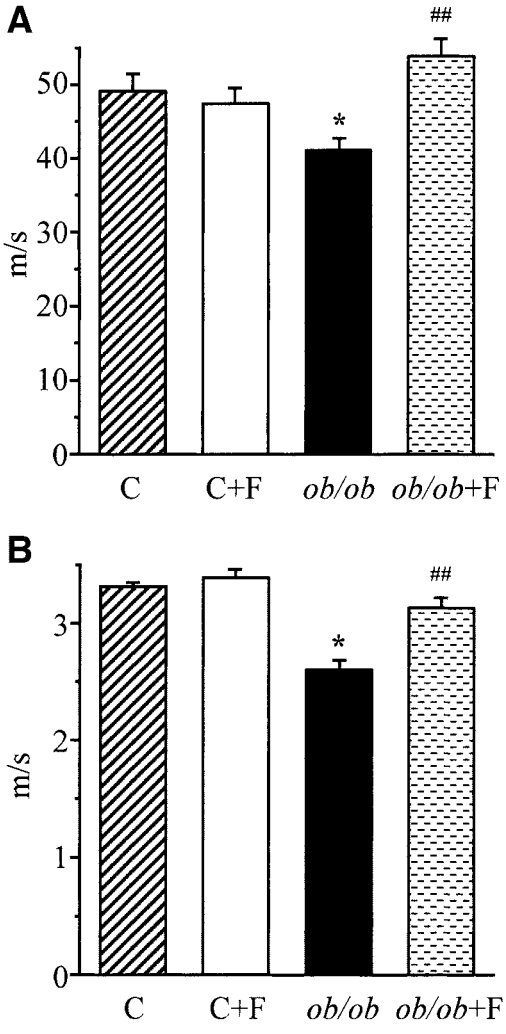

FIG. 1. Final sciatic MNCVs (*A*) and hind-limb digital SNCVs (*B*) in nondiabetic control (C) and *ob/ob* mice with and without fidarestat (F) treatment. Means ± SE, n = 10–15 per group. *$P < 0.01$ vs. nondiabetic control mice; ##$P < 0.01$ vs. untreated *ob/ob* mice.

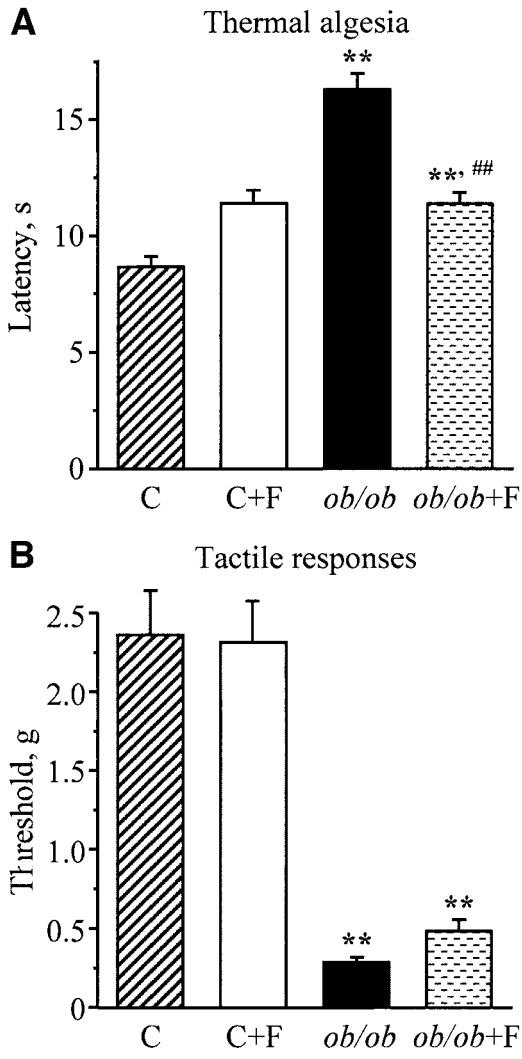

FIG. 2. Paw withdrawal latencies in response to thermal noxious stimuli (*A*) and tactile response thresholds in response to stimulation with flexible von Frey filaments (*B*) in nondiabetic control (C) and *ob/ob* mice with or without fidarestat (F) treatment. Means ± SE, n = 12–21 per group. **$P < 0.01$ vs. nondiabetic control mice; ##$P < 0.01$ vs. untreated *ob/ob* mice.

fidarestat-treated *ob/ob* mice preserved normal MNCV. In a similar fashion, hind-limb digital SNCV was reduced by 22% in *ob/ob* mice compared with nondiabetic controls (Fig. 1*B*), and this reduction was essentially prevented by fidarestat. Fidarestat did not affect MNCV or SNCV in nondiabetic control mice.

The latency of hind-paw withdrawal in response to radiant heat was increased by 88% in *ob/ob* mice compared with nondiabetic controls ($P < 0.01$), which is consistent with clearly manifest thermal hypoalgesia (Fig. 2*A*). Fidarestat partially (to 131% of control value, $P < 0.01$ vs. nondiabetic controls and $P < 0.01$ vs. untreated diabetic group) prevented a diabetes-induced increase in paw withdrawal latency. Of interest, paw withdrawal latency in nondiabetic control animals treated with fidarestat was 32% higher than in the corresponding untreated group.

Another sensory abnormality developing in *ob/ob* mice was tactile allodynia. Tactile withdrawal threshold in response to light touch with flexible von Frey filaments was reduced 8.2-fold in *ob/ob* mice compared with nondiabetic controls ($P < 0.01$; Fig. 2*B*). Tactile response

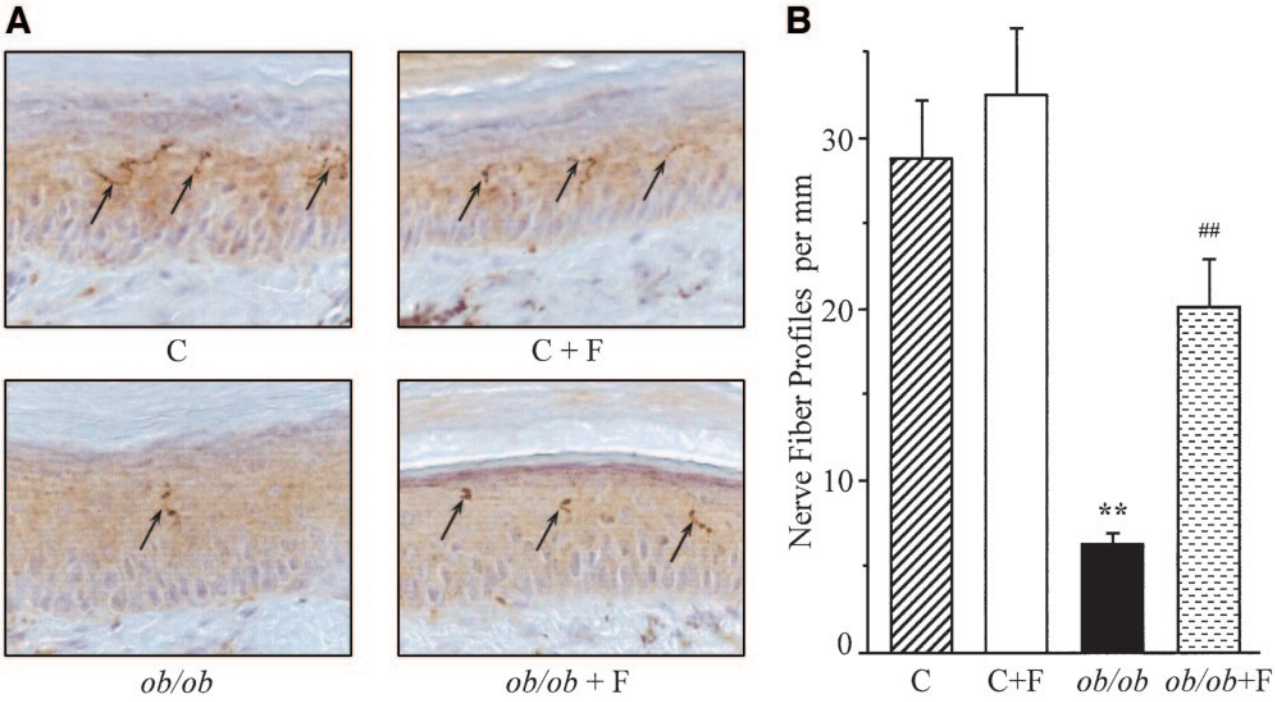

FIG. 3. Intraepidermal nerve fiber profiles in nondiabetic control (C) and *ob/ob* mice with and without fidarestat (F) treatment. *A*: Representative images, original magnification ×200. *B*: Skin fiber density. Means ± SE, $n = 8$–18 per group. **$P < 0.01$ vs. nondiabetic control mice; ##$P < 0.01$ vs. untreated *ob/ob* mice.

thresholds were 1.7-fold higher in *ob/ob* mice treated with fidarestat compared with the corresponding untreated group; however, the difference between fidarestat-treated and untreated *ob/ob* mice did not achieve statistical significance ($P = 0.44$). Furthermore, tactile response thresholds remained 4.9-fold lower in fidarestat-treated *ob/ob* mice compared with nondiabetic controls ($P < 0.01$). Fidarestat did not affect tactile response thresholds in the nondiabetic control group.

INFD was reduced by 78% in *ob/ob* mice compared with nondiabetic controls ($P < 0.01$; Fig. 3). Fidarestat essentially (to 72% of control value, $P < 0.01$ vs. untreated *ob/*ob mice and $P = 0.06$ vs. nondiabetic controls) prevented intraepidermal nerve fiber loss in *ob/ob* mice, without affecting this variable in control mice.

Nitrotyrosine immunoreactivity was increased by 78% in the sciatic nerve of *ob/ob* mice compared with nondiabetic controls (Fig. 4*A* and *B*), and this increase was prevented by fidarestat treatment. Fidarestat did not affect nitrotyrosine immunoreactivity in nondiabetic control mice. The number of the sciatic nerve poly(ADP-ribose)–positive nuclei was approximately twofold greater in *ob/ob* mice compared with nondiabetic controls ($P < 0.01$; Fig. 4*C* and *D*). No significant differences in the numbers of sciatic nerve poly(ADP-ribose)–positive nuclei were found between fidarestat-treated *ob/ob* mice and nondiabetic controls. Fidarestat did not affect poly(ADP-ribose) immunoreactivity in nondiabetic control mice. The similar patterns were observed in the spinal cord (Fig. 5) and DRGs (Fig. 6). In both sites, nitrotyrosine and poly(ADP-ribose) immunoreactivities were increased in *ob/ob* mice compared with nondiabetic controls ($P < 0.01$ for all comparisons). No significant differences in the spinal cord or DRG nitrotyrosine immunoreactivities or the numbers of poly(ADP-ribose)–positive nuclei were found between fidarestat-treated *ob/ob* mice and nondiabetic controls. Fidarestat did not affect nitrotyrosine or poly(ADP-ribose) immunoreactivities in the spinal cord and DRGs of nondiabetic control mice.

DISCUSSION

Recent clinical studies suggest that subjects with impaired glucose tolerance and obesity have increased risk for developing motor and sensory nerve conduction slowing and small sensory nerve fiber neuropathy (23–26). Obesity is clearly associated with increased prevalence of neuropathy in overt type 1 and type 2 diabetes (27,28). Pathogenetic mechanisms underlying PDN developing in the absence of fasting hyperglycemia (pre-diabetes) or under conditions of mild hyperglycemia in type 2 diabetes are poorly studied. Neurological and neurovascular deficits associated with type 2 diabetes have been described in sucrose-fed Otsuka Long-Evans Tokushima fatty (OLETF) rats (14), Goto-Kakizaki and BBZDR/Wor rats (15,16), and Zucker obese and Zucker diabetic fatty rats (12,13). Our findings indicate that leptin-deficient (*ob/ob*) mice with moderate hyperglycemia, hyperinsulinemia, and obesity (17,18) develop MNCV and SNCV deficits, thermal hypoalgesia, tactile allodynia, and epidermal sensory fiber loss, which are characteristic of human subjects with diabetes, and thus represent a valuable animal model of PDN of type 2 diabetes and obesity. This model has a number of advantages over existing animal models of type 2 diabetic neuropathy mentioned above. Whereas *ob/ob* mice have clearly manifest thermal hypoalgesia, i.e., condition observed in human subjects with PDN (3), BBZDR/Wor rats (15) and Zucker diabetic fatty rats (13) have persistent thermal hyperalgesia, which is a transient phenomenon in PDN in humans (29). In addition, blood glucose concentrations often achieve a very high level, ~30 mmol/l, in Zucker diabetic fatty rats (13), which makes the patholog-

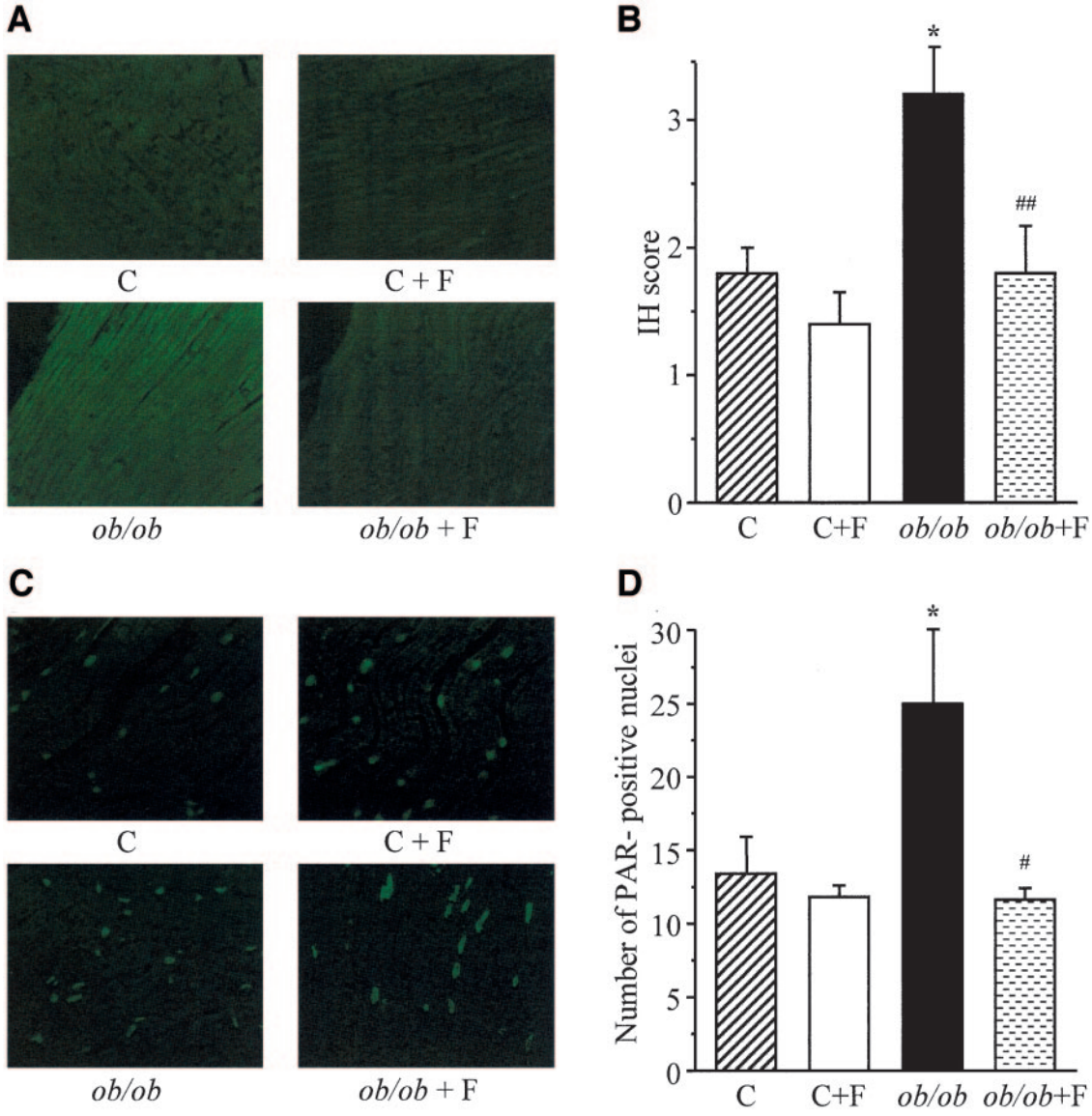

FIG. 4. Representative microphotographs of immunofluorescent staining of nitrotyrosine (*A*) and poly(ADP-ribose) (*C*) in sciatic nerves of nondiabetic control (C) and *ob/ob* mice with and without fidarestat (F) treatment. Magnification ×50. Scores of nitrotyrosine immunofluorescence (*B*) and the numbers of poly(ADP-ribose)–positive nuclei (*D*) in sciatic nerves of nondiabetic control mice and *ob/ob* mice with and without fidarestat treatment. Means ± SE, $n = 5$ per group. **$P < 0.01$ vs. nondiabetic control mice; ##$P < 0.01$ vs. untreated *ob/ob* mice.

ical condition in this model very different from type 2 diabetes. In contrast, nonfasting blood glucose concentrations in *ob/ob* mice typically do not exceed 20 mmol/l. OLETF rats develop nerve conduction deficit and peripheral nerve sorbitol pathway intermediate accumulation only after an extended (~8 weeks) feeding of sucrose to achieve severe hyperglycemia (14). In contrast, *ob/ob* mice developed clearly manifest motor and sensory nerve conduction slowing and peripheral nerve sorbitol pathway intermediate accumulation when fed a regular mouse diet to maintain moderate hyperglycemia. Goto-Kakizaki and Zucker obese rats better suit the experimental studies of neuropathy of pre-diabetes rather than of type 2 diabetes, as both models either do not develop overt fasting hyperglycemia (Goto-Kakizaki rats [15]) or develop it very late (~40 weeks of age) after a decline in β-cell function (Zucker obese rats [12]).

The severities of MNCV and SNCV deficits and thermal hypoalgesia in *ob/ob* mice were quite similar to those demonstrated in rats and mice with type 1 (streptozotocin-induced) diabetes (9,30 and I.G.O., V.V.L., unpublished observations). In addition, *ob/ob* mice clearly developed manifest tactile allodynia, a condition in which a light touch is perceived as painful. This phenomenon is observed in a considerable proportion (from 30% [31] to 47% [26]) of human subjects with diabetes and, so far, has not been described in mouse models of PDN. The severity of allodynia as determined by reduction in threshold of response to light touch with flexible von Frey filaments is quite comparable in 11-week-old *ob/ob* mice and rats with an 8-week duration of streptozotocin-induced diabetes (30).

Historically, small-caliber nerve fiber degeneration has not been evaluated in either human subjects with diabetes or animal models due to a lack of objective measures. Emerging new techniques such as corneal confocal microscopy, a reiterative, rapid, noninvasive in vivo imaging technique for quantitative assessment of degeneration and

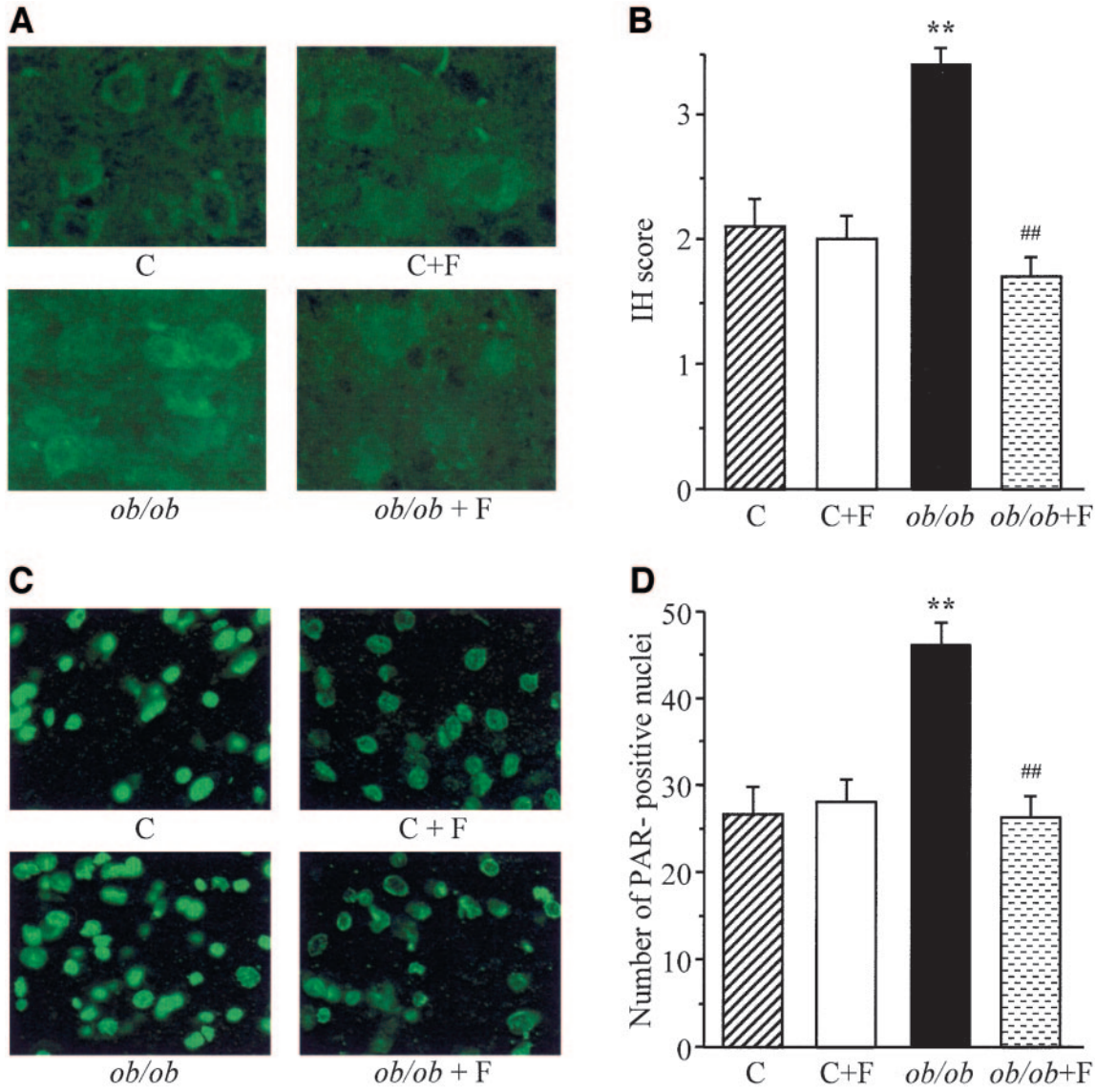

FIG. 5. Representative microphotographs of immunofluorescent staining of nitrotyrosine (*A*) and poly(ADP-ribose) (*C*) in the spinal cord of nondiabetic control (C) and *ob/ob* mice with and without fidarestat (F) treatment. Magnification ×100. Scores of nitrotyrosine immunofluorescence (*B*) and the numbers of poly(ADP-ribose)–positive nuclei (*D*) in the spinal cord of nondiabetic control mice and *ob/ob* mice with and without fidarestat treatment. Means ± SE, n = 7–16 per group. **P < 0.01 vs. nondiabetic control mice; ##P < 0.01 vs. untreated *ob/ob* mice.

regeneration of corneal nerve fibers (32), and skin biopsy with visualization and quantitation of epidermal nerve fibers (21,33,34) generated enormous potential for better understanding the mechanisms underlying small nerve fiber degeneration, a phenomenon that may ultimately lead to a complete loss of sensory function and is a major cause of foot amputation. Recent studies revealed that subjects with both type 1 and type 2 diabetes, but not those with metabolic syndrome, display epidermal nerve fiber loss (33–37). In our study, 11-week-old *ob/ob* mice developed a dramatic (78%) reduction in INFD compared with age-matched nondiabetic controls. Such a dramatic loss of epidermal nerve fibers probably reflects a synergistic effect of hyperglycemia and obesity. Note, like human subjects with metabolic syndrome (37), high-fat–fed mice with impaired glucose tolerance and obesity, but without overt hyperglycemia, do not display any epidermal fiber loss (I.G.O., V.R.D., V.V.L., unpublished observations). Moreover, a severe reduction in INFD in *ob/ob* mice exceeded that observed in streptozotocin-induced diabetic mice with an 8- to 12-week duration of diabetes and had more severe hyperglycemia but no obesity (~50%) (V.R.D., V.V.L., I.G.O., unpublished observations).

In evaluating amenability of PDN in *ob/ob* mice to pathogenetic treatment, we have chosen the AR inhibitor fidarestat for the following reasons. First, *ob/ob* mice display evidence of increased sorbitol pathway activity in the peripheral nerve. Second, numerous findings suggest that increased AR activity is the major "upstream" mechanism that accounts for or provides the important contribution to numerous diabetes-induced abnormalities in peripheral nervous system and other tissue sites for diabetes complications. During the last 20 years, increased AR activity was found to result in *myo*-inositol depletion and decrease in Na^+/K^+ ATP-ase activity (38), NAD^+/NADH redox changes (39), alterations in arachidonic acid metabolism (40), depletion of nerve growth factor and nerve growth factor–regulated neuropeptides (41,42), as well as ciliary neurotrophic factor (43), oxidative-nitrosative stress (44), and, recently, activation of mitogen-

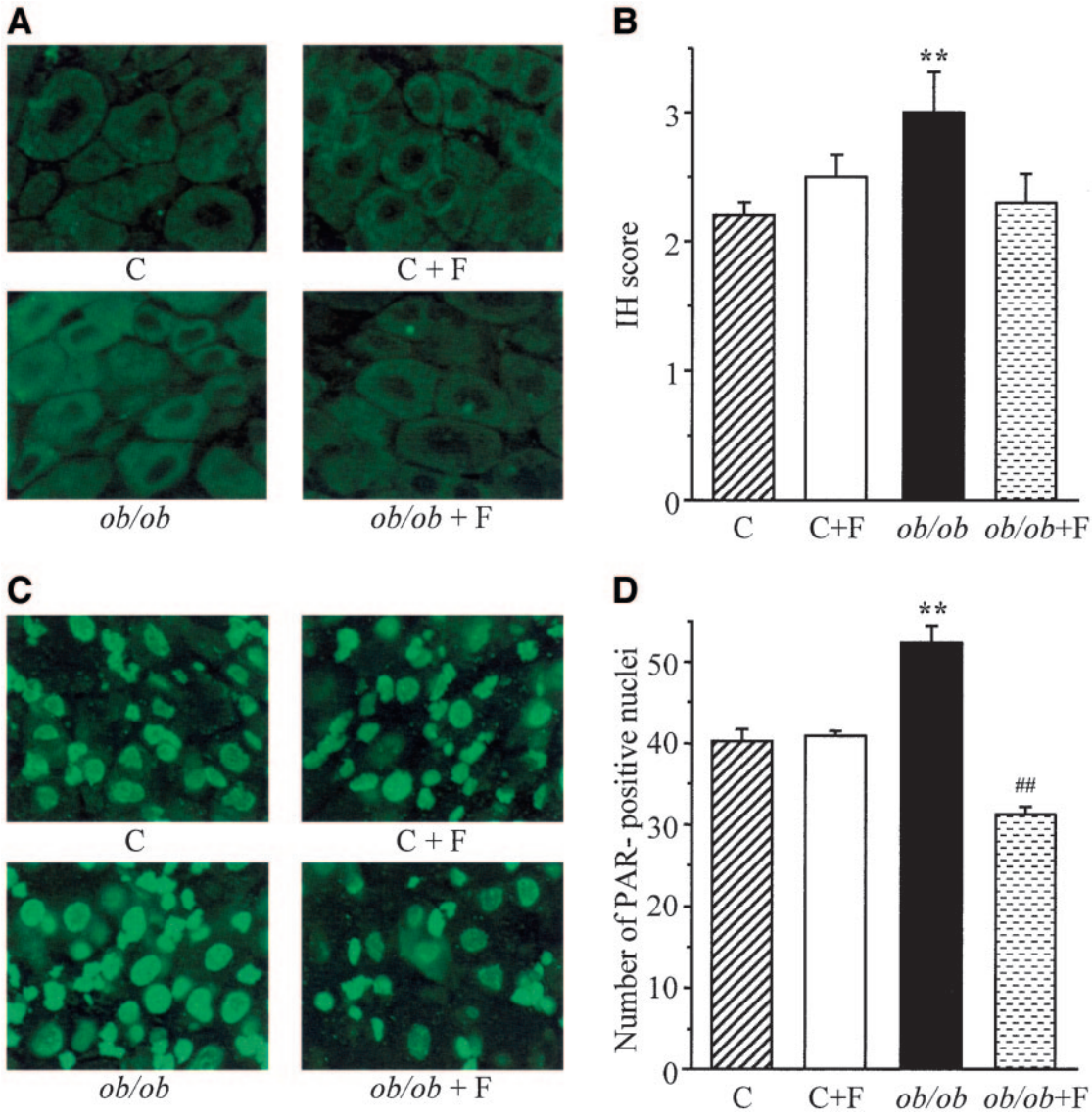

FIG. 6. Representative microphotographs of immunofluorescent staining of nitrotyrosine (*A*) and poly(ADP-ribose) (*C*) in the DRGs of nondiabetic control (C) and *ob/ob* mice with and without fidarestat (F) treatment. Magnification ×100. Scores of nitrotyrosine immunofluorescence (*B*) and the numbers of poly(ADP-ribose)–positive nuclei (*D*) in the DRGs of nondiabetic control mice and *ob/ob* mice with and without fidarestat treatment. Means ± SE, n = 5–18 per group. **P < 0.01 vs. nondiabetic control mice; ##P < 0.01 vs. untreated *ob/ob* mice.

activated protein kinases (45), poly(ADP-ribose) polymerase (44), and cyclooxygenase-2 (K. Ramos, N. Calcutt, unpublished observations). Third, AR inhibition or gene deficiency resulted in prevention and correction of functional and morphological abnormalities of PDN in streptozotocin-induced diabetic rats and mice (4,5,19,39,46). Furthermore, several clinical trials with different AR inhibitors revealed that robust inhibition of the enzyme activity is accompanied by a statistically significant increase in nerve conduction velocity and myelinated fiber density, as well as improvement of subjective symptoms of PDN (including numbness, spontaneous pain, sensation of rigidity, paresthesia in the sole upon walking, heaviness in the foot, and hypesthesia) (47–50). In the present study, AR inhibition with fidarestat resulted in complete or partial prevention of peripheral nerve sorbitol pathway intermediate accumulation, motor and sensory nerve conduction slowing, and thermal hypoalgesia in 11-week-old *ob/ob* mice. Furthermore, we obtained the first evidence of the efficacy of an AR inhibitor treatment in preventing small sensory nerve fiber degeneration characteristic for PDN and maintaining normal INFD. Note that beneficial effects of fidarestat on INFD in *ob/ob* mice were consistent with alleviation of thermal hypoalgesia, a functional correlate of small sensory nerve fiber degeneration. Alleviation of thermal hypoalgesia with the AR inhibitor fidarestat treatment is in line with previous studies with other AR inhibitors in the streptozotocin-induced diabetic rat model (30). Furthermore, alleviation of sensory neuropathy and, in particular, intraepidermal nerve fiber loss in our experimental study is consistent with improvement of subjective symptoms of PDN, i.e., numbness, sensation of rigidity, heaviness in the foot, and others, in the fidarestat clinical trial (48). Of interest, whereas tactile allodynia in streptozotocin-induced diabetic rats was totally nonresponsive to an AR inhibitor treatment (30), tactile response thresholds in fidarestat-treated *ob/ob* mice were ~1.7-fold higher than in the corresponding untreated group. This difference, however, was minor compared with an approximate eightfold in-

crease in tactile sensitivity in *ob/ob* mice compared with nondiabetic controls. The biochemical mechanisms underlying tactile allodynia are not understood; of interest, in the streptozotocin-induced diabetic rat model, poly(ADP-ribose) polymerase inhibition (20), but not AR inhibition (30), resulted in partial restoration of normal sensitivity to light touch. Perhaps a better understanding of diabetes-induced allodynia may be achieved by utilizing both functional (tactile response thresholds) and anatomical (Meissner corpuscle counts at the dermal-to-epidermal junction) assessment of this condition in PDN-related studies, including those addressing the role for AR. Of note, recent experimental (51,52) and clinical studies (50) have demonstrated *1*) the important role for AR in pathological conditions, others than diabetes, and *2*) the best efficacy of an AR inhibitor treatment in subjects with good glycemic control. Thus, current understanding of the metabolic function of sorbitol pathway is incomplete, which impedes the progress in identifying its role in disease, including PDN.

Evidence for an important role of free radicals and oxidants in PDN (9,10,53,54), including PDN in humans (55), is emerging. Our findings indicate that *ob/ob* mice have enhanced oxidative-nitrosative stress, manifest by increased nitrotyrosine and poly(ADP-ribose) immunoreactivities in peripheral nerve, spinal cord, and DRGs. An AR inhibitor treatment prevented nitrotyrosine and poly-(ADP-ribose) accumulation in all three tissue sites of PDN. The latter is consistent with *1*) AR localization in rodent peripheral nerve, spinal cord, and DRGs (56,57) and *2*) numerous findings (rev. in [44]) indicating that increased AR activity is localized upstream consequent to oxidative-nitrosative stress and poly(ADP-ribose) polymerase activation in tissue sites for diabetes complications.

In conclusion, the leptin-deficient *ob/ob* mouse is a new animal model of neuropathy of type 2 diabetes and obesity that develops both large motor and sensory fiber and small sensory fiber PDN, offers a number of advantages over existing animal models, and responds to pathogenetic treatment. The results support the role for increased AR activity in functional and structural changes of PDN in type 2 diabetes.

ACKNOWLEDGMENTS

This study was supported by an American Diabetes Association research grant and a Sanwa Kagaku Kenkyusho grant (both to I.G.O.).

REFERENCES

1. National Institutes of Diabetes and Digestive and Kidney Diseases: *Diabetes in America*. 2nd ed. Bethesda, Maryland, National Institutes of Diabetes and Digestive and Kidney Diseases, 1995 (NIH publ. no. 95-1468)
2. Boulton AJ: The diabetic foot: from art to science: the 18th Camillo Golgi Lecture. *Diabetologia* 47:1343–1353, 2004
3. Calcutt NA: Potential mechanisms of neuropathic pain in diabetes. *Int Rev Neurobiol* 50:205–228, 2002
4. Cameron NE, Cotter MA, Basso M, Hohman TC: Comparison of the effects of inhibitors of aldose reductase and sorbitol dehydrogenase on neurovascular function, nerve conduction and tissue polyol pathway metabolites in streptozotocin-diabetic rats. *Diabetologia* 40:271–281, 1997
5. Nakamura J, Kato K, Hamada Y, Nakayama M, Chaya S, Nakashima E, Naruse K, Kasuya Y, Mizubayashi R, Miwa K, Yasuda Y, Kamiya H, Ienaga K, Sakakibara F, Koh N, Hotta N: A protein kinase C-β–selective inhibitor ameliorates neural dysfunction in streptozotocin-induced diabetic rats. *Diabetes* 48:2090–2095, 1999
6. Obrosova IG, Van Huysen C, Fathallah L, Cao X, Stevens MJ, Greene DA: Evaluation of alpha(1)-adrenoceptor antagonist on diabetes-induced changes in peripheral nerve function, metabolism, and antioxidative defense. *FASEB J* 14:1548–1558, 2000
7. Cheng C, Zochodne DW: Sensory neurons with activated caspase-3 survive long-term experimental diabetes. *Diabetes* 52:2363–2371, 2003
8. Calcutt NA, Allendoerfer KL, Mizisin AP, Middlemas A, Freshwater JD, Burgers M, Ranciato R, Delcroix JD, Taylor FR, Shapiro R, Strauch K, Dudek H, Engber TM, Galdes A, Rubin LL, Tomlinson DR: Therapeutic efficacy of sonic hedgehog protein in experimental diabetic neuropathy. *J Clin Invest* 111:507–514, 2003
9. Obrosova IG, Li F, Abatan OI, Forsell MA, Komjati K, Pacher P, Szabo C, Stevens MJ: Role of poly(ADP-ribose) polymerase activation in diabetic neuropathy. *Diabetes* 53:711–720, 2004
10. Obrosova IG, Mabley JG, Zsengeller Z, Charniauskaya T, Abatan OI, Groves JT, Szabo C: Role for nitrosative stress in diabetic neuropathy: evidence from studies with a peroxynitrite decomposition catalyst. *FASEB J* 19:401–403, 2005
11. Nigro J, Osman N, Dart AM, Little PJ: Insulin resistance and atherosclerosis. *Endocr Rev* 27:242–259, 2006
12. Oltman CL, Coppey LJ, Gellett JS, Davidson EP, Lund DD, Yorek MA: Progression of vascular and neural dysfunction in sciatic nerves of Zucker diabetic fatty and Zucker rats. *Am J Physiol Endocrinol Metab* 289:E113–E122, 2005
13. Li F, Abatan OI, Kim H, Burnett D, Larkin D, Obrosova IG, Stevens MJ: Taurine reverses neurological and neurovascular deficits in Zucker diabetic fatty rats. *Neurobiol Dis* 22:669–676, 2006
14. Nakamura J, Koh N, Sakakibara F, Hamada Y, Wakao T, Sasaki H, Mori K, Nakashima E, Naruse K, Hotta N: Diabetic neuropathy in sucrose-fed Otsuka Long-Evans Tokushima fatty rats: effect of an aldose reductase inhibitor, TAT. *Life Sci* 60:1847–1857, 1997
15. Murakawa Y, Zhang W, Pierson CR, Brismar T, Ostenson CG, Efendic S, Sima AA: Impaired glucose tolerance and insulinopenia in the GK-rat causes peripheral neuropathy. *Diabetes Metab Res Rev* 18:473–483, 2002
16. Kamiya H, Murakawa Y, Zhang W, Sima AA: Unmyelinated fiber sensory neuropathy differs in type 1 and type 2 diabetes. *Diabetes Metab Res Rev* 21:448–458, 2005
17. Coleman DL: Diabetes-obesity syndromes in mice. *Diabetes* 31 (Suppl. 1):1–6, 1982
18. Houseknecht KL, Portocarrero CP: Leptin and its receptors: regulators of whole-body energy homeostasis. *Domest Anim Endocrinol* 15:457–475, 1998
19. Kato N, Mizuno K, Makino M, Suzuki T, Yagihashi S: Effects of 15-month aldose reductase inhibition with fidarestat on the experimental diabetic neuropathy in rats. *Diabetes Res Clin Pract* 50:77–85, 2000
20. Ilnytska O, Lyzogubov VV, Stevens MJ, Drel VR, Mashtalir N, Pacher P, Yorek MA, Obrosova IG: Poly(ADP-Ribose) polymerase inhibition alleviates experimental diabetic sensory neuropathy. *Diabetes* 55:1686–1694, 2006
21. Malmberg AB, Mizisin AP, Calcutt NA, von Stein T, Robbins WR, Bley KR: Reduced heat sensitivity and epidermal nerve fiber immunostaining following single applications of a high-concentration capsaicin patch. *Pain* 111:360–367, 2004
22. Obrosova IG, Fathallah L, Lang HJ, Greene DA: Evaluation of a sorbitol dehydrogenase inhibitor on diabetic peripheral nerve metabolism: a prevention study. *Diabetologia* 42:1187–1194, 1999
23. Becker J, Nora DB, Gomes I, Stringari FF, Seitensus R, Panosso JS, Ehlers JC: An evaluation of gender, obesity, age and diabetes mellitus as risk factors for carpal tunnel syndrome. *Clin Neurophysiol* 113:1429–1434, 2002
24. Miscio G, Guastamacchia G, Brunani A, Priano L, Baudo S, Mauro A: Obesity and peripheral neuropathy risk: a dangerous liaison. *J Peripher Nerv Syst* 10:354–358, 2005
25. Singleton JR, Smith AG, Russell J, Feldman EL: Polyneuropathy with impaired glucose tolerance: implications for diagnosis and therapy. *Curr Treat Options Neurol* 7:33–42, 2005
26. Vinik AI, Suwanwalaikorn S, Stansberry KB, Holland MT, McNitt PM, Colen LE: Quantitative measurement of cutaneous perception in diabetic neuropathy. *Muscle Nerve* 18:574–584, 1995
27. Szelag B, Wroblewski M, Castenfors J, Henricsson M, Berntorp K, Fernlund P, Sundkvist G: Obesity, microalbuminuria, hyperinsulinemia, and increased plasminogen activator inhibitor 1 activity associated with parasympathetic neuropathy in type 2 diabetes. *Diabetes Care* 22:1907–1908, 2002
28. De Block CE, De Leeuw IH, Van Gaal LF: Impact of overweight on chronic microvascular complications in type 1 diabetic patients. *Diabetes Care* 28:1649–1655, 2005
29. Dyck PJ, Dyck PJ, Larson TS, O'Brien PC, Velosa JA: Patterns of quantitative sensation testing of hypoesthesia and hyperalgesia are predictive of

diabetic polyneuropathy: a study of three cohorts: Nerve Growth Factor Study Group. *Diabetes Care* 23:510–517, 2000
30. Calcutt NA, Freshwater JD, Mizisin AP: Prevention of sensory disorders in diabetic Sprague-Dawley rats by aldose reductase inhibition or treatment with ciliary neurotrophic factor. *Diabetologia* 47:718–724, 2004
31. Bastyr EJ 3rd, Price KL, Bril V, the MBBQ Study Group: Development and validity testing of the neuropathy total symptom score-6: questionnaire for the study of sensory symptoms of diabetic peripheral neuropathy. *Clin Ther* 27:1278–1294, 2005
32. Malik RA, Kallinikos P, Abbott CA, van Schie CH, Morgan P, Efron N, Boulton AJ: Corneal confocal microscopy: a non-invasive surrogate of nerve fibre damage and repair in diabetic patients. *Diabetologia* 46:683–688, 2003
33. Sumner CJ, Sheth S, Griffin JW, Cornblath DR, Polydefkis M: The spectrum of neuropathy in diabetes and impaired glucose tolerance. *Neurology* 60:108–111, 2003
34. Pittenger G, Burkus N, McNulty P, Basta B, Vinik A: Intraepidermal nerve fibers are indicators of small-fiber neuropathy in both diabetic and nondiabetic patients. *Diabetes Care* 27:1974–1979, 2004
35. Shun CT, Chang YC, Wu HP, Hsieh SC, Lin WM, Lin YH, Tai TY, Hsieh ST: Skin denervation in type 2 diabetes: correlations with diabetic duration and functional impairments. *Brain* 127:1593–1605, 2004
36. Boucek P, Havrdova T, Voska L, Lodererova A, Saudek F, Lipar K, Janousek L, Adamec M, Sommer C: Severe depletion of intraepidermal nerve fibers in skin biopsies of pancreas transplant recipients. *Transplant Proc* 37:3574–3575, 2005
37. Pittenger G, Mehrabyan A, Simmons K, Rice A, Barlow P, Vinik A: Small fiber neuropathy is associated with the metabolic syndrome. *Metabolic Syndrome and Related Disorders* 3:113–121, 2005
38. Stevens MJ, Dananberg J, Feldman EL, Lattimer SA, Kamijo M, Thomas TP, Shindo H, Sima AA, Greene DA: The linked roles of nitric oxide, aldose reductase and, (Na+,K+)-ATPase in the slowing of nerve conduction in the streptozotocin diabetic rat. *J Clin Invest* 94:853–859, 1994
39. Obrosova IG, Van Huysen C, Fathallah L, Cao XC, Greene DA, Stevens MJ: An aldose reductase inhibitor reverses early diabetes-induced changes in peripheral nerve function, metabolism, and antioxidative defense. *FASEB J* 16:123–125, 2002
40. Kuruvilla R, Eichberg J: Depletion of phospholipid arachidonoyl-containing molecular species in a human Schwann cell line grown in elevated glucose and their restoration by an aldose reductase inhibitor. *J Neurochem* 71:775–783, 1998
41. Ohi T, Saita K, Furukawa S, Ohta M, Hayashi K, Matsukura S: Therapeutic effects of aldose reductase inhibitor on experimental diabetic neuropathy through synthesis/secretion of nerve growth factor. *Exp Neurol* 151:215–220, 1998
42. Diemel LT, Stevens EJ, Willars GB, Tomlinson DR: Depletion of substance P and calcitonin gene-related peptide in sciatic nerve of rats with experimental diabetes: effects of insulin and aldose reductase inhibition. *Neurosci Lett* 137:253–256, 1992
43. Mizisin AP, Calcutt NA, DiStefano PS, Acheson A, Longo FM: Aldose reductase inhibition increases CNTF-like bioactivity and protein in sciatic nerves from galactose-fed and normal rats. *Diabetes* 46:647–652, 1997
44. Obrosova IG, Pacher P, Szabo C, Zsengeller Z, Hirooka H, Stevens MJ, Yorek MA: Aldose reductase inhibition counteracts oxidative-nitrosative stress and poly(ADP-ribose) polymerase activation in tissue sites for diabetes complications. *Diabetes* 54:234–242, 2005
45. Price SA, Agthong S, Middlemas AB, Tomlinson DR: Mitogen-activated protein kinase p38 mediates reduced nerve conduction velocity in experimental diabetic neuropathy: interactions with aldose reductase. *Diabetes* 53:1851–1856, 2004
46. Ho ECM, Lam KSL, Chen YS, Yip JCW, Arvindakshan M, Yamagishi S-I., Yagihashi S, Oates PJ, Ellery CA, Chung SSM, Chung SK: Aldose reductase–deficient mice are protected from delayed motor nerve conduction velocity, increased c-Jun NH_2-terminal kinase activation, depletion of reduced glutathione, increased superoxide accumulation, and DNA damage. *Diabetes* 55:1946–1953, 2006
47. Greene DA, Arezzo JC, Brown MB: Effect of aldose reductase inhibition on nerve conduction and morphometry in diabetic neuropathy: Zenarestat Study Group. *Neurology* 53:580–591, 1999
48. Hotta N, Toyota T, Matsuoka K, Shigeta Y, Kikkawa R, Kaneko T, Takahashi A, Sugimura K, Koike Y, Ishii J, Sakamoto N, the SNK-860 Diabetic Neuropathy Study Group: Clinical efficacy of fidarestat, a novel aldose reductase inhibitor, for diabetic peripheral neuropathy: a 52-week multicenter placebo-controlled double-blind parallel group study. *Diabetes Care* 24:1776–1782, 2001
49. Bril V, Buchanan RA: Long-term effects of ranirestat (AS-3201) on peripheral nerve function in patients with diabetic sensorimotor polyneuropathy. *Diabetes Care* 29:68–72, 2006
50. Hotta N, Akanuma Y, Kawamori R, Matsuoka K, Oka Y, Shichiri M, Toyota T, Nakashima M, Yoshimura I, Sakamoto N, Shigeta Y: Long-term clinical effects of epalrestat, an aldose reductase inhibitor, on diabetic peripheral neuropathy: the 3-year, multicenter, comparative Aldose Reductase Inhibitor-Diabetes Complications Trial. *Diabetes Care* 29:1538–1544, 2006
51. Hwang YC, Kaneko M, Bakr S, Liao H, Lu Y, Lewis ER, Yan S, Ii S, Itakura M, Rui L, Skopicki H, Homma S, Schmidt AM, Oates PJ, Szabolcs M, Ramasamy R: Central role for aldose reductase pathway in myocardial ischemic injury. *FASEB J* 18:1192–1199, 2004
52. Hallam K, Gomez T, Li Q, Ananthakrishnan R, Yan S, Schmidt AM, Ramasamy R: Polyol pathway inhibition improves age-related vascular dysfunction in rats (Abstract). *Exp Biol* C276:738.18, 2006
53. Cameron NE, Tuck Z, McCabe L, Cotter MA: Effect of the hydroxyl radical scavenger, dimethylthiourea, on peripheral nerve tissue perfusion, conduction velocity and nociception in experimental diabetes. *Diabetologia* 44:1161–1169, 2001
54. Coppey LJ, Gellett JS, Davidson EP, Dunlap JA, Lund DD, Yorek MA: Effect of antioxidant treatment of streptozotocin-induced diabetic rats on endoneurial blood flow, motor nerve conduction velocity, and vascular reactivity of epineurial arterioles of the sciatic nerve. *Diabetes* 50:1927–1937, 2001
55. Ametov AS, Barinov A, Dyck PJ, Hermann R, Kozlova N, Litchy WJ, Low PA, Nehrdich D, Novosadova M, O'Brien PC, Reljanovic M, Samigullin R, Schuette K, Strokov I, Tritschler HJ, Wessel K, Yakhno N, Ziegler D, the SYDNEY Trial Study Group: The sensory symptoms of diabetic polyneuropathy are improved with α-lipoic acid: the SYDNEY trial. *Diabetes Care* 26:770–776, 2003
56. Gabbay KH, O'Sullivan JB: The sorbitol pathway: enzyme localization and content in normal and diabetic nerve and cord. *Diabetes* 17:239–243, 1968
57. Llewelyn JG, Thomas PK, Mirrlees DJ: Aldose reductase activity and myo-inositol levels in sciatic nerve and dorsal root ganglia of the diabetic mutant mouse [C57/BL/Ks (db/db)]. *Metabolism* 40:1084–1087, 1991